Neuroscience Letters 684 (2018) 29–34

Contents lists available at ScienceDirect

Neuroscience Letters

journal homepage: www.elsevier.com/locate/neulet

Research article

Repeated mild shaking of neonates induces transient cerebral microhemorrhages and anxiety-related behavior in adult rats

Yasushi Kawamata[a], Ayuka Ehara[b], Tsuyoshi Yamaguchi[b], Yoshiteru Seo[c], Kazutaka Shimoda[a], Shuichi Ueda[b,*]

[a] Department of Psychiatry, Dokkyo Medical University School of Medicine, Mibu, Tochigi, 321-0293, Japan
[b] Department of Histology and Neurobiology, Dokkyo Medical University School of Medicine, Mibu, Tochigi, 321-0293, Japan
[c] Department of Regulatory Physiology, Dokkyo Medical University School of Medicine, Mibu, Tochigi, 321-0293, Japan

ARTICLE INFO

Keywords:
Shaken baby syndrome
Animal model
Microhemorrhage
Susceptibility weighted imaging
Iron histochemistry
Anxiety

ABSTRACT

Growing evidence suggests that neonatal cerebral microhemorrhages (MHs) are implicated in neuropsychiatric diseases in adults. Although animal studies have identified the progression of the underlying mechanisms of MHs, few studies have investigated the histopathology and behavioral outcomes. In this study, we created an experimental rat model of MHs using a new experimental device for repeated mild shaking brain injury (SBI) in the neonatal period and examined temporal changes in MHs using susceptibility weighted imaging (SWI) and iron histochemistry. SWI demonstrated transient MHs in the gray matter of the cerebral cortex and hippocampus in injured rats. Iron histochemical staining demonstrated leakage of iron and iron-positive cells surrounding MHs. This staining pattern lasted for a long time and continued after disappearance of hemorrhagic signals on SWI. These data suggested the presence of iron-associated gray matter injury after MHs. In the open field test, these injured rats showed anxiety-related behavior as adults. This model may be useful for exploring the underlying mechanisms of changes that occur after MHs and the behavioral outcomes of repeated mild SBI in early development.

1. Introduction

Abusive head trauma in childhood, known as “shaken baby syndrome” (SBS), is considered to increase the risk for psychiatric disorders in adolescents and adults [1,2]. In SBS, characteristic pathological features of violent head shaking are various combinations of subdural, subarachnoid, and intracerebral hemorrhages and skull fractures [3]. Hemorrhages of various sizes can occur in SBS brains, and over 30% of SBS victims die due to such hemorrhages [3]. However, small hemorrhages and/or those without severe neurological signs are difficult to accurately diagnose and so far have received less attention. To investigate the pathological changes in the developing brain following shaking brain injury (SBI) and its relationship to changes in behavior, several animal models for SBS have been developed [4,5]. In these models, rodents are advantageous for studies of molecular and histopathological mechanisms following shaking insults [6].

Improved and advanced magnetic resonance imaging techniques such as susceptibility weighted imaging (SWI) can detect cerebral microhemorrhages (MHs) [7]. In SWI studies in humans, MHs are an imaging biomarker of “small vessel disease” in elderly people, whereas the presence of hemosiderin (a marker of earlier sustained hemorrhages) in the brain has been used as a prognostic indicator in preterm infants [8]. Although MHs have been demonstrated with SWI after traumatic brain injury (TBI) in model animals [9], no study has reported MHs after SBS and/or SBI in models. In the present study, we designed and built a new apparatus for repeated mild SBI to produce MHs in neonatal brains. Using SWI and histochemical staining, temporal changes in MHs were studied following neonatal repeated SBI.

Hemorrhages in the neonatal brain cause more severe injuries than in the adult brain [10]. Several mechanisms have been proposed for hemorrhage-induced tissue injury. Iron is a central player in such mechanisms. When red blood cells (RBCs) degenerate, hemoglobin liberates oxidized heme and further degrades into iron, bilirubin, and carbon monoxide. Iron can lead to formation of reactive oxygen species, which can promote cytotoxicity [11]. To identify the changes in iron distribution after SBI, we further examined changes in iron in the SBI model using modified Perls staining [12]. Finally, the effects of SBI on long-term emotional outcomes were examined in the novel open field test.

* Corresponding author at: Department of Histology and Neurobiology, Dokkyo Medical University School of Medicine, Tochigi, 321-0293, Japan.
E-mail address: shu-ueda@dokkyomed.ac.jp (S. Ueda).

https://doi.org/10.1016/j.neulet.2018.06.059
Received 12 May 2018; Received in revised form 19 June 2018; Accepted 30 June 2018
Available online 02 July 2018

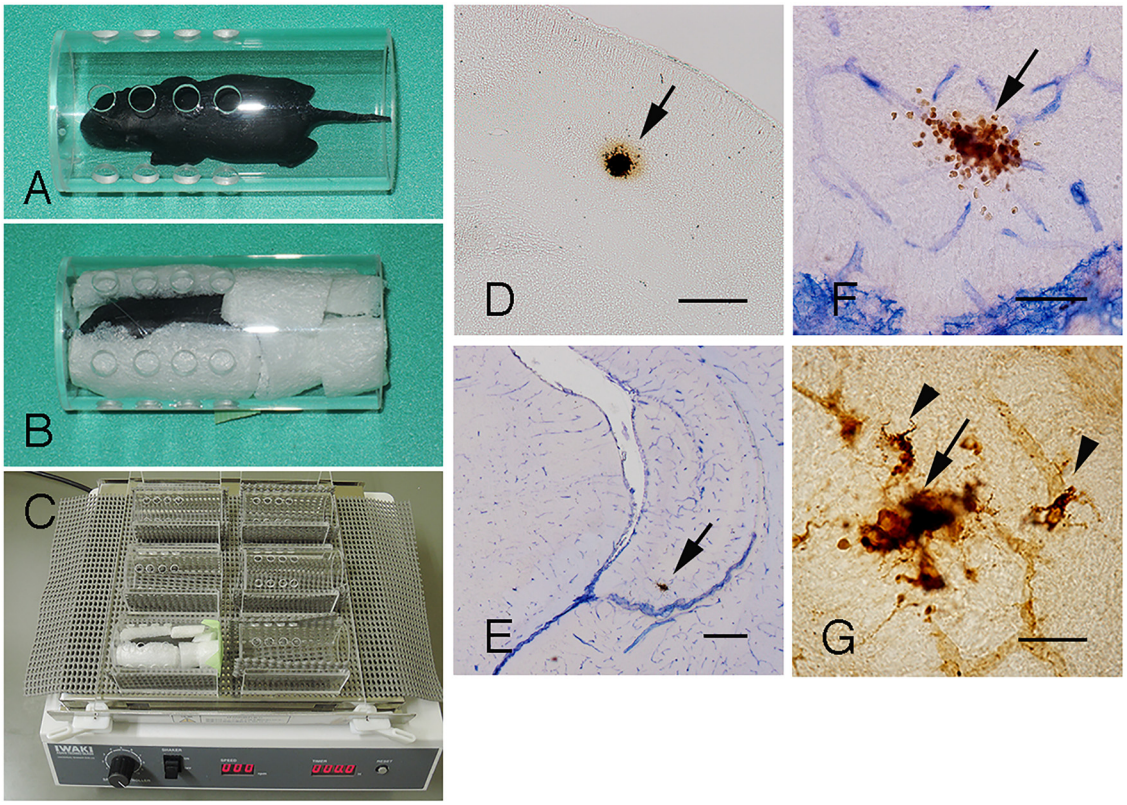

Fig. 1. Shaking apparatus (A–C). (A) The whole body mold for P3 rats was made with epoxy resin. The surface of the mold was painted black. The mold was inserted into the holding chamber, which was made with transparent polyvinyl chloride. (B) The pup is fixed in the mold with cushioning materials made of plant starch and polyvinyl alcohol, and the mold was placed in the chamber. (C) The shaking apparatus is composed of an anchor plate and shaker. The anchor plate is fixed on the shaker with a rubber sheet. The chambers are fixed on the anchor plate. (D–G) Histochemical staining of coronal sections through the parietal cortex (D) and hippocampus (E–G). (D) DAB histochemical staining indicates a focal hemorrhage (arrow) in the parietal corte × 2 h after shaking P3 rats. (E, F) Double labeling to identify extra-vessel bleeding. Endothelial cells of blood vessels are immunohistochemically stained with RECA-1 (blue), and red blood cells were stained with DAB (brown). (E) Focal hemorrhage (arrow) in the hippocampus 2 h after shaking P3 rats. (F) High magnification view of the focal hemorrhage in E. (G) High magnification view of the hippocampus stained with the modified Perls method without H_2O_2 pretreatment 2 h after shaking P7 rats. A cluster of red blood cells (arrow) and iron-positive cells (arrowheads) are evident. Scale bars = 400 μm (D, E), 100 μm (F), and 40 μm (G)..

2. Materials and methods

2.1. Animals

Timed-pregnant female Sprague-Dawley rats were purchased from Japan Charles River Lab Inc. (Tsukuba, Japan) and were housed under controlled conditions of temperature (22 ± 2 °C), humidity (50–60%), and a regular 12-h light-dark cycle with ad libitum access to food and water. The date of birth was considered postnatal day 0 (P0). All experimental procedures were performed following approval by the Animal Welfare Committee of Dokkyo Medical University School of Medicine and were conducted in accordance with the National Institutes of Health Guide for the Care and Use of Laboratory Animals.

2.2. Apparatus

The shaking apparatus was composed of three parts: the holding chamber for holding an individual rat pup; the anchor plate that connected the chamber and shaker; and the shaker (Fig. 1A–C). The holding chamber was a transparent cylinder made of polyvinyl chloride with an outside diameter of 40 mm, inside diameter of 38 mm, and length of 80 mm (Fig. 1A). The body of the chamber had 12 openings for ventilation. One side of the chamber was closed, and the other side opened with a hatch. At the time of shaking, the pup was fixed in the chamber with cushioning materials made of plant starch and polyvinyl alcohol (Fig. 1B). The anchor plate was a transparent plate (300 mm × 350 mm × 5 mm) made of polyvinyl chloride with attachments for 10 holding chambers at once. The shaker was a common laboratory shaker (SHK-U3, IWAKI Co. LTD., Tokyo, Japan). The pistons moved back and forth horizontally at speeds of 0–250 revolutions per minute (rpm) (Fig. 1C).

2.3. Experimental design

To evaluate the intensity of shaking, male P3-14 rat pups were anesthetized with 2% isoflurane or sevoflurane in air and were shaken for 60 s and allowed to rest for 60 s; these steps were repeated five times per day (S group). The control (C group) pups were placed in the chamber without shaking for the same experimental period under anesthesia. Based on the shaking frequencies of previous rodent models of SBS [4,5], we used 250 rpm (26.16 rad/s, 4.1 Hz) for the intensity (frequency) of shaking in this study. Throughout the experiments, to prevent hypoxia-asphyxia stress, changes in skin color and breathing were carefully observed during and after shaking [5]. After shaking, all pups were subsequently returned to their dam until weaning (P21). Offspring were then placed in a cage with 2–3 animals per cage. The time-course of the present experiment is shown in Suppl. Fig.1.

2.4. Tissue preparation and immunohistochemistry

To examine the presence of hemorrhages in the brain, 2 h after shaking P3 and P7 rats in the S group and pups in the age-matched C group were used for the first step of histological investigation. Under deep anesthesia with pentobarbital, these rats were transcardially

perfused with physiological saline, followed by 4% paraformaldehyde in 0.1 M phosphate buffer (PB, pH 7.4) at 4 °C. Brains were removed from the skulls and placed in 30% sucrose in 0.1 M PB. The brains from P3 rats were rapidly embedded in 10% gelatin and further fixed in the same fixative. All brains were frozen in powdered dry ice, and serial 40-μm-thick frontal sections were prepared using a cryostat. These serial sections were divided into six groups. To identify the presence of hemorrhages, the first series of sections was incubated with 3, 3′-diaminobenzidine (DAB) to visualize endogenous peroxidase in RBCs. Moreover, to clarify the location of RBCs and the cerebral blood vessels, the second series of sections was immunohistochemically stained with rat endothelial cell antigen 1 (RECA-1) to label blood vessels and histochemically stained for endogenous peroxidase to label RBCs. Briefly, for double labeling, the sections were washed in 0.3% Triton X in 0.05 M Tris-buffered saline (TBS; pH 7.6) and then in normal goat serum in TBS to block non-specific reactions. The sections were incubated with mouse anti-rat RECA-1 (1:20000, SEROTEC, Oxford, UK) at 4 °C overnight. After rinsing three times in TBS, the sections were incubated with alkaline phosphatase-conjugated goat anti-mouse IgG secondary antibody (1:500, Sigma Aldrich, St. Louis, MO, USA) for 60 min at room temperature. After rinsing three times in TBS, the sections were incubated for 5 min in 0.1 M Tris HCl (pH 8.2) containing Vector Blue substrate (Vector Lab, Burlingame, CA, USA), and then the sections were incubated with DAB in Tris HCl (pH 7.6) with 0.003% of H_2O_2 to visualize RBCs. The stained sections were mounted in Immuno mount (Thermo Scientific, Pittsburgh, PA, USA).

2.5. Magnetic resonance imaging (MRI)

To investigate MHs or edematous changes in living animals (P4, P6, and P12 of the S group), we employed MRI. Because of the size of MHs, we used SWI, which visualizes differences in volume magnetic susceptibility between tissues [13]. Using high-field MRI (7 T AVANCE III, Bruker Biospin, Ettlingen, Germany), even a small amount of deoxyhemoglobin can be detected as a low signal intensity compared with surrounding intact tissues. Thus, we can detect a small hemorrhage in the cerebral cortex. The original image was obtained with an 18-mm surface coil (Doty Scientific Inc., Columbia, SC, USA) and by T_1-weighted gradient-echo imaging (2D-T_{1w}) with a field of view of 19.2 × 19.2 mm^2, data matrix of 256 × 256, slice thickness of 0.5 mm, seven slices with separation of 0.7 mm, repetition time of 250 ms, echo-time of 15 ms, and flip angle of 45°. SWI processing was applied with a mask weighting value of 3 and Gaussian broadening of 1 mm. During MRI measurement, each pup was anesthetized with 1% sevoflurane in a gas mixture of $O_2/CO_2/N_2O$ delivered through a face mask at a rate of 0.4 L min^{-1}. Body temperature was monitored using a fluorescence thermometer (AMOS FX-8000-210, Anritsu Meter, Tokyo, Japan). Pups were subsequently returned to their dam, and the spots of MHs were traced for several days.

2.6. Modified Perls staining

Under deep anesthesia with pentobarbital, P4, P7, P35 (5 weeks, 5 W), P8W, and P10 W rats of the S and C groups were transcardially perfused with physiological saline, followed by 4% paraformaldehyde in 0.1 M PB (pH 7.4) at 4 °C. The tissue preparations were similar to the immunohistochemical procedures. One series of sections was pretreated with 1% H_2O_2 in phosphate-buffered saline (PBS), and another series of sections was directly incubated with Perls solution. The sections were stained according to the modified Perls method [12]. The sections were then washed in PBS, mounted on slides, dehydrated, and coverslipped. Two investigators independently evaluated the number of rats with MHs and the number of MHs in the brain of P3, P7, P5 W and P8-10 W rats from the S group.

2.7. Novel open field test

Maternal separation affects offspring behavior [14]. In the open field test, we used naive control pups (N group) that had not been manipulated and had not experienced maternal separation until P21, in addition to the C group. With the open field apparatus, behavioral analysis was performed as previously reported [15]. Briefly, P10 W male rats from each group were exposed to the novel open field for 15 min, and the horizontal locomotion (number of total squares crossed) and the frequencies of rearing (defined as standing upright on the hind legs) were recorded.

2.8. Statistical analysis

Data are presented as means ± standard error of the mean (SEM). All statistical measurements were carried out using Stat View (Abacus Concepts, Inc., Berkeley, CA, USA). For the number of MHs and the open field test, significant differences between the groups were evaluated with the unpaired *t*-test. A value of $p < 0.05$ was considered significant.

3. Results

No significant difference was found in body weight between the control group and experimental group during P3-P8W (Suppl. Fig. 2), and all rats used in this experiment survived until sacrifice. At the macroscopic level, no obvious differences were seen between the S and C groups, including disruption of the brain surface or subdural hemorrhages. However, DAB histochemical staining at the microscopic level showed multiple focal hemorrhages in the gray matter and subarachnoid hemorrhages at 2 h after shaking in all P3 and P7 S group rats. In the gray matter, hemorrhages were usually observed in the prefrontal, parietal, temporal, cingulate, and insular cortices (Fig. 1D), hippocampus (Fig. 1E–G), thalamus, cerebellum, and brainstem. The size of the hemorrhages varied from 50 to 300 μm in diameter. However, no hemorrhages over 300 μm in diameter were found. Thus, we designated these hemorrhages as MHs in the rats. The size of MHs tended to be larger in the cerebral cortex and cerebellum than in other areas. The number of MHs was significantly higher in P7 rats than in P3 rats (Table 1). Occasionally, the corpus callosum (CC) and internal and external capsules contained hemorrhagic features. Double staining (blood vessels and RBCs) showed extravasation of RBCs, indicating disruption of cerebral blood vessels near the HMs (Fig. 1F). These blood vessels stained with RECA-1 immunohistochemistry and averaged about 7.6 ± 0.7 in diameter. Thus, the disrupted vessels were recognized as capillaries including pre-capillary arterioles and post-capillary venules. In control rats of all ages and P5 W, P8W, and P10 W S group rats, MHs were not detected throughout the brain (Table 1).

MHs showed decreased signal intensity in SWI. In four of six P4 pups in the S group, MHs were detected in the parietal and temporal cortices

Table 1
The number of rats with hemorrhages and the number of hemorrhages per rat.

Postnatal day (P) Total number (n)	Number of rats with hemorrhages			Number of hemorrhages per rat
	Gray matter		White matter	
	Cortex	Hippocampus		Mean ± SEM
P3 (n = 11)	11	9	2	5.09 ± 0.49
P7 (n = 12)	12	10	2	12.5 ± 0.94*
P35 (n = 6)	ND	ND	ND	0
P56 - 70 (n = 6)	ND	ND	ND	0

Analysis with DAB staining and modified Perls staining of sections.
ND: not detected.
* $p < 0.0001$ versus P3.

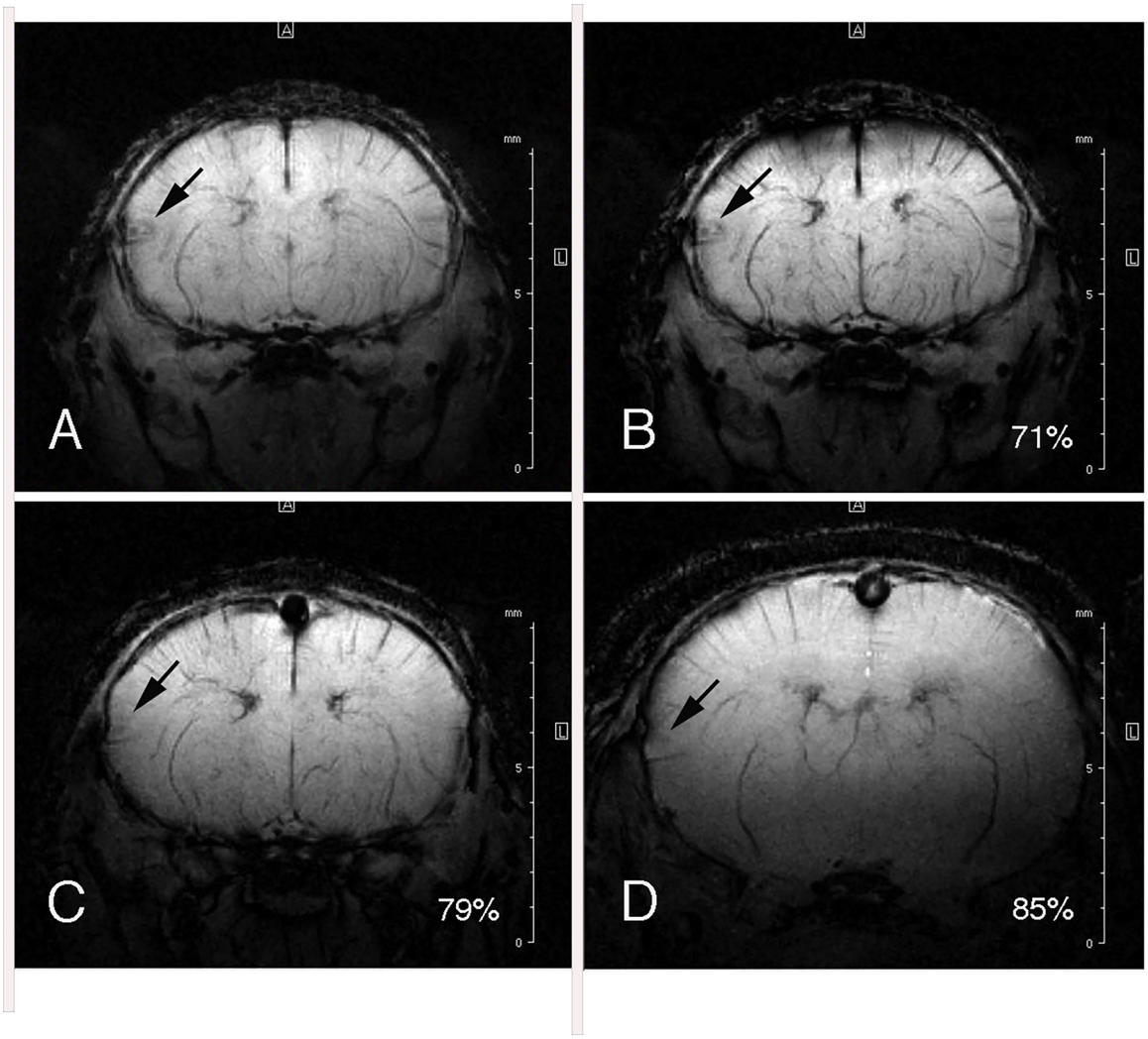

Fig. 2. Representative in vivo T2* (A) and SWI (B–D) coronal sections through the parietal cortex of the same S group rat at P4 (A, B), P6 (C), and P12 (D). Image intensities of SWI of ROIs (30 pixels) were measured in the hemorrhagic area (arrow) (ROIh) and in the non-hemorrhagic area (ROIn) nearby. (B–D) The number in the right corner indicates the % of ROIh/ROIn. Hypointensity signal in the parietal cortex (arrow) of P4 changes gradually over time.

(Fig. 2A and B). Although these pups underwent shaking manipulation every day, MHs that appeared at P4 gradually disappeared over time (Fig. 2C and D). However, new MHs occurred in other areas.

Iron staining patterns in the C group rats were consistent with those of previous reports [12]. After pretreatment with H_2O_2 to quench endogenous peroxidase activity of RBCs, modified Perls staining showed several patterns of iron reaction products (punctate iron reaction products, perivascular iron accumulation, and intracellular iron accumulation) similar to patterns seen in the neonatal hypoxic-ischemic brain injury model [16]. Adjacent sections were stained using the modified Perls method without H_2O_2 pretreatment, staining both hemorrhages and iron reactive products in the same section. Following this procedure, iron reactive products appeared mainly near the MHs. Abnormal distribution patterns of iron staining were classified into three types: hemorrhage (H) type, consisting mainly of RBCs (Fig. 3A); mixed (M) type, consisting of H, iron-positive cells, and iron reaction products (Figs. 1G and 3B); and perivascular (P) type, consisting of iron-positive cells and punctate iron reaction products without RBCs (Fig. 3C) near the vessels. In P3 rats, H type staining was predominantly observed. Beginning at P7, M type staining was increased. At P35, only P type staining existed in the gray matter.

The numbers of line crossings and rearing events in the open field test were significantly reduced in the S group (crossing 107.3 ± 5.7, rearing 26.8 ± 2.2, n = 14) compared with those in the C (crossing 258.4 ± 8.1, rearing 57.2 ± 2.7, n = 14) and N groups (crossing 280.3 ± 13.6, rearing 47.7 ± 2.9, n = 6) ($p < 0.0001$). No significant differences in line crossing or rearing were observed between the C and N groups (crossing $p = 0.16$, rearing $p = 0.051$) (Fig. 4).

4. Discussion

This study aimed to introduce a rat new model for SBS with mild brain injury. The new shaking device accomplished this objective. Neonatal repeated SBI using this device successfully created transient MHs in the brain, especially in the gray matter of the cerebral cortex and hippocampus. Another major finding of the present study was that neonatal repeated SBI induced iron leakage surrounding MHs, causing long-lasting iron deposits and leading to emotional abnormalities in adults.

Different from previous rodent SBS models [4,5], the present SBI animals showed a survival rate of 100% and no significant weight difference between the S and C groups throughout the experimental period. Using anesthetized P6 rat pups, Smith et al. [4] studied the effects of SBI on the brain and demonstrated that shaking alone does not produce significant brain hemorrhaging in infant rats. However, the additional insult of hypoxia (hypoxic air, 8% O_2/92% N_2) combined with shaking produces massive hemorrhages in the brain. Using P8 mice, Bonnier et al. [5] reported that horizontal rotational shaking

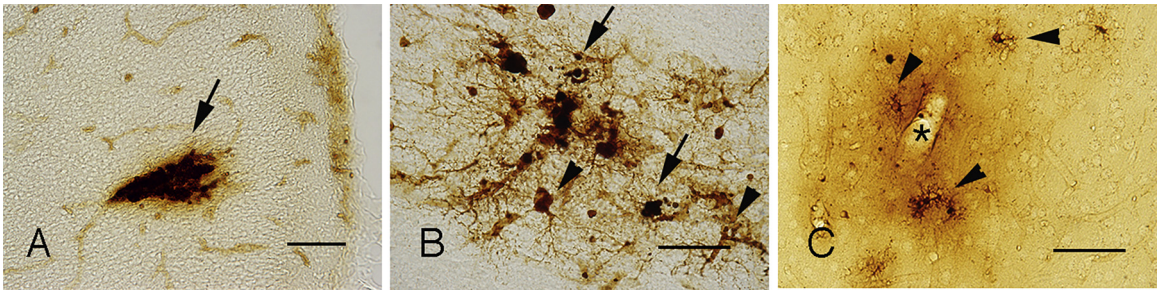

Fig. 3. Coronal sections through the prefrontal (A, B) and parietal cortices (C) stained with the modified Perls method without H_2O_2 pretreatment in S group rats. (A) Hemorrhage type staining pattern in a P3 rat. (B) Mixed type staining consisting of red blood cells (RBCs, arrows), iron-positive cells (arrowheads), and punctate iron reaction product in a P7 rat. (C) Perivascular (P) type staining consisting of enlarged capillaries (asterisk), iron-positive cells (arrowheads), and punctate iron reaction product in a P35 rat. Scale bar = 100 μm (A–C).

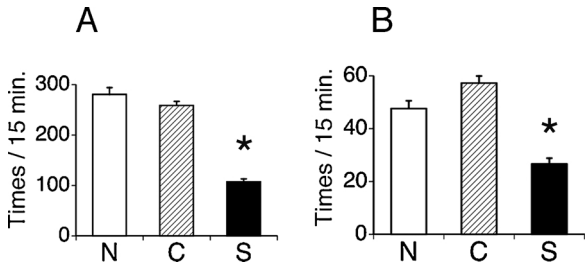

Fig. 4. Number of line crossings during 15 min (A) and number of rearing events during 15 min (B) in the different groups of rats in the novel open field. Shaken group rats (S) show a significant reduction in horizontal (line crossing) and vertical (rearing) activities compared to naive (N) and control (C) group rats. *$p < 0.0001$ versus N and C.

without hypoxia produces focal white matter hemorrhages and cysts in the CC and cerebellar medulla after the injury. Recently, in another SBS mouse model, Wang et al. [17] showed that parenchymal hemorrhages are not observed in the brain after injury. Instead they observed subarachnoid hemorrhages and increased blood-brain barrier (BBB) permeability. Similar to the rat model of closed head TBI using the weight-drop method [9], the present SWI study demonstrated multiple hemorrhages in the brain after SBI. Furthermore, the present histochemical analysis indicated the presence of intracerebral MHs in all P3 and P7 rats 2 h after injury. In agreement with a previous study [9], we confirmed that the detection sensitivity of MHs was higher with histochemical staining than with SWI. In the present model, most MHs were located in the gray matter and were rarely observed in the white matter. The locational difference of MHs has been reported in an MRI study of humans. MHs after TBI predominantly occur in the deep white matter, whereas gray matter MHs are frequently associated with stroke [18].

Shaking is a mechanical type of injury in which the brain shifts violently back and forth in the skull, causing superficial pial vessels to burst [4]. The present rat model first demonstrated the appearance of SBI-induced parenchymal MHs in the cerebral cortex and hippocampus due to disruption of capillaries. As the number of MHs increased from P3 to P7, the appearance of MHs seemed to increase with daily shaking sessions for at least 5 days. A recently developed photodestruction method for subcortical blood vessels produces a cortical gray matter-specific stroke injury. Using this technique, laser pulse energy-dependent stroke models have been reported [19]. Photodisruption of subsurface cortical capillaries leads to MHs in the exposed area, impaired blood flow in downstream vessels, extravasation of blood plasma, and local hypoxia near the injured vessels [19]. Iron accumulation is a sensitive indicator of hypoxic-ischemic injury [16]. A specific iron histochemical staining pattern was reported after hypoxic-ischemic insults in neonatal (P7) rats [16]. Due to the increased BBB permeability, the capillaries of P7 rats have been known to be vulnerable to ischemic insults [16]. A similar staining pattern, especially recognized as M type staining, was focally observed in the present study. This strongly suggests iron accumulation near the MHs due to focal hypoxic-ischemic insults. Thus, we hypothesized that focal ischemia occurred around MHs. Furthermore, erythrocyte lysis after a hemorrhage increases nonheme iron in the brain that is seen as an enhanced Perls reaction [20]. Following iron histochemistry in the current study, the distribution of the M type was similar to that of the H type, and the M type included various degrees of MHs and iron-positive cells. Together, these data indicate progression from the H type to the M type, although transition to the P type was not identified. Microglia/macrophages react rapidly with hemorrhagic insults, increase in number, and transform to an activated phenotype near the hemorrhage [21]. Because activated microglia show a strong iron-positive reaction [16], the iron-positive cells in the M type staining are likely activated microglia. To clarify the temporal changes in MHs and their surrounding areas in this model, detailed histochemical analyses are needed.

In the open field test, decreased ambulation (horizontal movements) and rearing behaviors indicate anxiety-related behavior in the rats. In adult rats, iron overload increases anxiety-related behavior, and excess iron accumulates at high levels in the hippocampus and basal ganglia [22]. Excess iron accumulation causes brain injury via formation of free radicals [11,20]. The hippocampus is involved in the neuronal circuits of anxiety [23] and is vulnerable to iron-induced oxidative stress [24]. Nanoscale intracortical injection of iron [25] and very mild TBI in the developing hippocampus [26] induce cortical and hippocampal dysfunction, respectively. Taken together, we hypothesize that local MHs in the hippocampus of the present model cause increased formation of iron-induced reactive oxygen species, which leads to long-lasting dysfunction of the hippocampus. Besides the hippocampus, MHs after SBI were frequently observed in the prefrontal cortex, another area involved in the neuronal circuit of anxiety [23]. Although cortical MHs temporarily inhibit neuronal activity in the surrounding area of the parietal cortex [27], the effects of MHs in the prefrontal cortex on neuronal activity related to anxiety-related behavior have not been elucidated. Additional physiological, molecular, and behavioral studies will provide useful information.

In conclusion, we show in a new rat SBS model that neonatal repeated shaking led to MHs and iron accumulation in the gray matter and can predispose the rats to anxiety-related behavior as adults. This experimental model provides new insight into the anxiety-prone state of children abused by shaking.

Conflict of interest

The authors declare no conflict of interest.

Acknowledgements

This study was funded by a Young Investigator Award (Grant No.

2016-10 for Y.K.) from Dokkyo Medical University. The authors are grateful to Ms. Shukuko Nihei for technical assistance and Ms. Fusae Terauchi for assistance in manuscript preparation.

Appendix A. Supplementary data

Supplementary material related to this article can be found, in the online version, at doi:https://doi.org/10.1016/j.neulet.2018.06.059.

References

[1] A.H. Whitaker, J.F. Feldman, J.M. Lorenz, F. McNicholas, P.W. Fisher, S. Shen, J. Pinto-Martin, D. Shaffer, N. Paneth, Neonatal head ultrasound abnormalities in preterm infants and adolescent psychiatric disorders, Arch. Gen. Psychiatry 68 (2011) 742–752.
[2] M.H. Teicher, J.A. Samson, C.M. Anderson, K. Ohashi, The effects of childhood maltreatment on brain structure, function and connectivity, Nat. Rev. Neurosci. 17 (2016) 652–666.
[3] A.C. Duhaime, T.A. Gennarelli, L.E. Thibault, D.A. Bruce, S.S. Margulies, R. Wiser, The shaken baby syndrome. A clinical, pathological, and biomechanical study, J. Neurosurg. 66 (1987) 409–415.
[4] S.L. Smith, E.D. Hall, Tirilazad widens the therapeutic window for riluzole-induced attenuation of progressive cortical degeneration in an infant rat model of the shaken baby syndrome, J. Neurotrauma 15 (1998) 707–719.
[5] C. Bonnier, B. Mesples, S. Carpentier, D. Henin, P. Gressens, Delayed white matter injury in a murine model of shaken baby syndrome, Brain Pathol. 12 (2002) 320–328.
[6] M.C. Morgani-Kossmann, E. Yan, N. Bye, Animal models of traumatic brain injury: is there an optimal model to reproduce human brain injury in the laboratory? Injury 41 (Suppl. 1) (2010) S10–S13.
[7] A. Charidimou, D.J. Werring, Cerebral microbleeds and cognition in cerebrovascular disease: an update, J. Neurol. Sci. 322 (2012) 50–55.
[8] F.T. de Bruine, S.J. Steggerda, A.A. van den Berg-Huysmans, L.M. Leijser, M. Rijken, M.A. van Buchem, G. van Wezel-Meijler, J. van der Grond, Prognostic value of gradient echo T2* sequences for brain MR imaging in preterm infants, Pediatr. Radiol. 44 (2014) 305–312.
[9] S. Kallakuri, S. Bandaru, N. Zakaria, Y. Shen, Z. Kou, L. Zhang, E.M. Haacke, J.M. Cavanaugh, Traumatic brain injury by a closed head injury device induces cerebral blood flow changes and microhemorrhages, J. Clin. Imaging Sci. 5 (2015) 52.
[10] M. Xue, M.R. Del Bigio, Injection of blood, thrombin, and plasminogen more severely damage neonatal mouse brain than mature mouse brain, Brain Pathol. 15 (2005) 273–280.
[11] G. Minhas, S. Modgil, A. Anand, Role of iron in ischemia-induced neurodegeneration: mechanisms and insights, Metab. Brain Dis. 29 (2014) 583–591.
[12] J.M. Hill, R.C. Switzer III, The regional distribution and cellular localization of iron in the rat brain, Neuroscience 11 (1984) 595–603.
[13] E.M. Haacke, Y. Xu, Y.C. Cheng, J.R. Reichenbach, Susceptibility weighted imaging (SWI), Magn. Reson. Med. 52 (2004) 612–618.
[14] J. McIntosh, H. Anisman, Z. Merali, Short- and long-periods of neonatal maternal separation differentially affect anxiety and feeding in adult rats: gender-dependent effects, Brain Res. Dev. Brain Res. 113 (1999) 97–106.
[15] W. Matsuda, A. Ehara, K. Nakadate, K. Yoshimoto, S. Ueda, Effects of environmental enrichment on the activity of the amygdala in micrencephalic rats exposed to a novel open field, Congenit. Anom. 58 (2018) 16–23.
[16] C. Palmer, S.L. Menzies, R.L. Roberts, G. Pavlick, J.R. Connor, Changes in iron histochemistry after hypoxic-ischemic brain injury in the neonatal rat, J. Neurosci. Res. 56 (1999) 60–71.
[17] G. Wang, Y.P. Zhang, Z. Gao, L.B.E. Shields, F. Li, T. Chu, H. Lv, T. Moriarty, X.M. Xu, X. Yang, C.B. Shields, J. Cai, Pathophysiological and behavioral deficits in developing mice following rotational acceleration-deceleration traumatic brain injury, Dis. Models Mech. 11 (2018).
[18] T. Imaizumi, K. Miyata, S. Inamura, I. Kohama, K.S. Nyon, T. Nomura, The difference in location between traumatic cerebral microbleeds and microangiopathic microbleeds associated with stroke, J. Neuroimaging 21 (2011) 359–364.
[19] N. Nishimura, C.B. Schaffer, B. Freidman, P.S. Tsai, P.D. Lyden, D. Kleinfeld, Targeted insult to subsurface cortical blood vessels using ultrashort laser pulses: three models of stroke, Nat. Methods 3 (2006) 99–108.
[20] J. Wu, Y. Hua, R.F. Keep, T. Nakamura, J.T. Hoff, G. Xi, Iron and iron-handling proteins in the brain after intracerebral hemorrhage, Stroke 34 (2003) 2964–2969.
[21] C.F. Chang, J. Wan, Q. Li, S.C. Renfroe, N.M. Heller, J. Wang, Alternative activation-skewed microglia/macrophages promote hematoma resolution in experimental intracerebral hemorrhage, Neurobiol. Dis. 103 (2017) 54–69.
[22] K. Maaroufi, M. Ammari, M. Jeljeli, V. Roy, M. Sakly, H. Abdelmelek, Impairment of emotional behavior and spatial learning in adult Wistar rats by ferrous sulfate, Physiol. Behav. 96 (2009) 343–349.
[23] P. Tovote, J.P. Fadok, A. Luthi, Neuronal circuits for fear and anxiety, Nat. Rev. Neurosci. 16 (2015) 317–331.
[24] K.M. Rodrigue, A.M. Daugherty, E.M. Haacke, N. Raz, The role of hippocampal iron concentration and hippocampal volume in age-related differences in memory, Cereb. Cortex 23 (2013) 1533–1541.
[25] A. Jo, C. Heo, T.H. Schwarz, M. Suh, Nanoscale intracortical iron injection induces chronic epilepsy in rodent, J. Neurosci. Res. 92 (2014) 389–397.
[26] Z. Yu, B. Morrison III, Experimental mild traumatic brain injury induces functional alteration of the developing hippocampus, J. Neurophysiol. 103 (2010) 499–510.
[27] F.A. Cianchetti, D.H. Kim, S. Dimiduk, N. Nishimura, C.B. Schaffer, Stimulus-evoked calcium transients in somatosensory cortex are temporarily inhibited by a nearby microhemorrhage, PloS One 8 (2013) e65663.